Indonesian Physical Review

Volume 7 Issue 1, January 2024
P-ISSN: 2615-1278, E-ISSN: 2614-7904

Effect of $Fe_3O_4/SiO_2/TiO_2$ Photocatalyst on Pollutant Management in Swamp Water

Beta Riana Liasari[1], Fitri Suryani Arsyad [1*], Assaidah[1], Ramlan[1], Siti Nur'aini[1], Balada Soerya[1]

[1] *Physics Study Program, Faculty of Mathematics and Natural Sciences, University of Sriwijaya*

Corresponding Authors E-mail: fitri_suryani@unsri.ac.id

Article Info

Article info:
Received: 29-08-2023
Revised: 02-11-2023
Accepted: 07-11-2023

Keywords:
Fe_3O_4; TiO_2; SiO_2

How To Cite:
B. R. Liasari, F. S. Arsyad, Ramlan, S. Nur'aini, and B. Soerya, "Effect of $Fe_3O_4/SiO_2/TiO_2$ Photocatalyst on Pollutant Management in Swamp Water", Indonesian Physical Review, vol. 7, no. 1, p 10-31, 2024.

DOI:
https://doi.org/10.29303/ipr.v7i1.271.

Abstract

Water is an essential source of life, thus regulating its purity is critical in daily living. Water has a high acid content (pH) and contains a variety of harmful chemical elements such as iron (Fe), copper (Cu), sulphate (SO_4), nitrate (NO_3), chloride (Cl), and other dangerous bacteria. The goal of this research is to create wastewater management such that it can be used by the community. The process involves creating Fe_3O_4 catalysts that have been modified using SiO_2 and TiO2. The application of dirty water employs $Fe_3O_4/SiO_2/TiO_2$ to bind contaminants in polluted water. The results of the photocatalyst process carried out by $Fe_3O_4/SiO_2/TiO_2$ reach 90% in 180 minutes of UV light irritation so that it can degrade water pollutants such as methylene orange.

Introduction

People's capacity to acquire clean water has become increasingly problematic in recent years [1], [2]. This is due to pollution from industrial, animal husbandry, farm, and domestic activities, which drastically decreases the quality of water in bodies of water such as lakes, rivers, marshes, and reservoirs [3], [4]. Swamp regions are one of the natural resources that can be used to generate growth, which is thought to be capable of increasing the rate of economic development and community welfare [5]. Aside from that, swamp water is water found in swamp and lowland areas, particularly in Sumatra and Kalimantan, that has the characteristics of a low pH (3-5) or high acidity level, yellowish brown color, and high levels of organic, iron, and manganese, but has the potential to be used as raw water through certain processes [6], [7].

In general, the water quality index indicates the quality of the environment surrounding bodies of water, including wetlands. Water quality is critical, given that water serves as a source of all life [8]. Organic waste is generated by human activities, particularly household, agricultural, and fishery waste, resulting in eutrophication and a deterioration in water quality. Pollution and shallowing also impact the functioning of aquatic ecosystems, the economy, and public health [9–11]. There are many contaminants in wastewater, but toxicity is only found over specified limits known as acceptable limits. The pollutants found in wastewater are determined by the nature of the industrial, agricultural, and municipal wastewater discharge operations. Water pollutants can be classified as inorganic, organic, or biological in nature [11–14]. Heavy metals are the most frequent inorganic water pollutants, and they are very poisonous and carcinogenic in nature. Furthermore, nitrates, sulfates, phosphates, fluorides, chlorides, and oxalates have some major negative effects [12], [15].

Heavy metal waste is a severe issue due to its adverse impact on humans and animals [16–20]. Heavy metals include lead, arsenic, cadmium, chromium, copper, zinc, mercury, iron, aluminum, nickel, barium, manganese, and beryllium [13], [21]. As the industry grows, more colored wastewater is released into the natural environment from factories (e.g., food processing plants, printing, and textile manufacturers). Colored wastewater discharged from these businesses may provide eco-toxic risks, resulting in potential bioaccumulation risks [22]. Pesticides, which include insecticides, herbicides, fungicides, polynuclear hydrocarbons (PAH), phenols, polychlorinated biphenyls, halogenated aromatic hydrocarbons, formaldehyde, polybrominated biphenyls, biphenyls, detergents, oils, and greases, cause toxic organic contamination. Normal hydrocarbons, alcohols, aldehydes, ketones, proteins, lignin, and medicines are also found in wastewater. Different types of bacteria that thrive in wastewater may be responsible for various diseases [23].

The availability of clean water for varied activities is the most difficult task for scholars and practitioners all around the world. As a consequence of the serious efforts of researchers all over the world on the subject of pollution control and management, a number of approaches with varied degrees of success have been created to manage water contamination [24]. Coagulation, foam flotation, filtration, ion exchange, sedimentation, solvent extraction, adsorption, electrolysis, chemical oxidation, disinfection, chemical deposition, and membrane processes are among them. However, this approach has its own drawbacks and limits [23], [25]. This procedure normally uses a lot of energy and can be complicated by moving pollutants between different fluids, wastes, and byproducts of wastewater treatment. It is critical for economic and social growth to identify gentler reaction conditions and effective catalysts to remove various contaminants from wastewater [26].

Photocatalysis is a procedure that uses light as an energy source to activate a catalyst that enhances the rate of a chemical reaction without being involved in the reaction [27].

Photocatalysis is a multifunctional phenomenon with numerous applications such as pollutant degradation, hydrogen production, carbon dioxide reduction, nitrogen fixation, microbial disinfection, and so on [28], [29]. Various semiconductors have been investigated for use as photocatalysts, including titanium (IV) oxide (TiO_2), zinc (II) oxide (ZnO), gallium arsenide, tungsten (VI) oxide (WO_3), gallium phosphide, and cadmium sulphide [30]. Apart from that, oxide minerals such as iron oxide (Fe_3O_4) and silica oxide (SiO_2) can be employed as photocatalyst materials. With mild conditions, a simple method, and green technology, photocatalysis can decompose organic contaminants in wastewater into water, carbon dioxide, or other tiny molecules, and decrease or oxidize inorganic pollutants into innocuous compounds [31]. Below are several studies that have made photocatalysts as controllers to overcome water pollution which can be seen in Tabel 1:

Tabel 1. Various types of photocatalysts have been modified to overcome water pollution.

Photocatalyst	Method	Treatment	Ref
MXene composite membrane	Low temperature chemical modification	Oil/water separation and dye removal in water	[32]
Hetero-conjunction composite $BiVO_4/FeVO_4$@rGO	Hydrothermal	Tetracycline (TC) and reduction of Cr (VI)	[33]
Magnetic composite of TiO_2-graphene	Sol-gel	Herbicide	[34]
Composite Ag@ZnO/BiOCl	Hydrothermal	Antibiotics	[35]
Oxygen deficient SnO_2 quantum dots (QDs)	Facile one-step	Oil in water	[36]
BiOCl nanosheet-decorated carbon quantum dot composite/carbonized eggshell membrane	Addition of BiOCl nanosheets to carbonized eggshell membrane (CEM)	Tetracycline hydrochloride (TC), Rhodamine B (RhB) dan o-nitrophenol (NP)	[37]
Hetero-conjunction scheme-S $BiOCl/CuBi_2O_4$ with a lack of oxygen	solvothermal	Nitric oxide	[38]
$Ag-Fe_3O_4/TiO_2$	Chemical reduction	Dye Degradation and H_2 Production in Light and Dark Conditions	[39]
Fe_3O_4/TiO_2	Hydrothermal	Methylene Blue	[40]
SiO_2/TiO_2	Sol-gel	Methylene Blue	[41]

Based on table 1, it shows various types of photocatalyst applications that can be used on waste in water systems. However, here we will focus more on the $Fe_3O_4/SiO_2/TiO_2$ composite synthesis method, namely using a relatively cheap and simple coprecipitation method which will greatly influence the quality of photocatalyst applications.

Theory

TiO_2 is a natural titanium oxide that is stable and corrosion-resistant [42-45]. TiO_2 is the most extensively employed photocatalyst in the degradation of organic pollutants due to its low cost, stability, toxicity, and environmental friendliness [46]-[48]. Although TiO_2 is traditionally considered low toxicity, the development of TiO_2 nanotechnology has resulted in greater human and environmental exposure, putting TiO_2 nanoparticles under toxicological scrutiny. Researchers are interested in TiO_2 photocatalysis because of its potential applications in environmental stewardship and pollution control. TiO_2 can be found in the structures of anatase, brookite, and rutile, as shown in Figure 1 and Table 2.

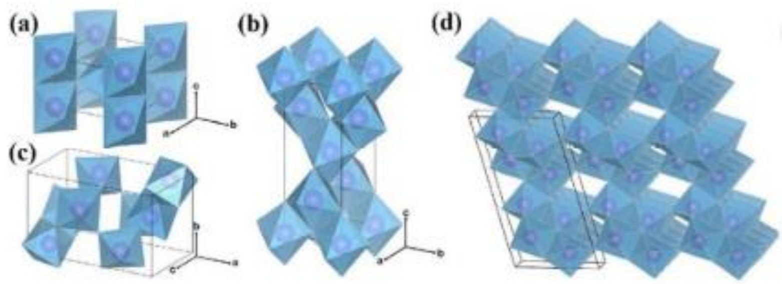

Figure 1. Polymorph crystal structure of TiO_2: a) Rutile, b) Anatase, c) Brookite and d) TiO_2(B)[49].

Although rutile is the most frequent form of TiO_2 with thermal stability, anatase TiO2 has increased photosensitive characteristics due to its good charge carrier mobility and higher number of surface hydroxyl groups [50]. TiO_2 based photocatalysis has become a feasible technology for a variety of applications, including the remediation of various environmental contaminants and environmentally friendly organic synthesis processes [51].

Table 2. TiO_2 Properties and Characteristics [51].

Characteristic	The structure of crystals	Density	Band gap (eV)	Adsorption of light (n/m)	Photocatalyst (mol/h)	Dielectric constant	Area enthalpy (J/m²)
Rutile	Tetragonal	4,13	3.0	<415	1.1×10^{-5}	6.62	1.93
Anatase	Tetragonal	3,79	3.2	<390	3.5×10^{-5}	6.04	1.34
Brokite	Ortorombik	3,99	3.2	-	-	-	1.66

Figure 1 depicts the TiO_2 photocatalyst. TiO_2's principal crystal modifications are anatase and rutile. Both structures are made up of TiO_6 octahedra with titanium ions in the centre and oxygen ions at the vertices. In the rutile polymorph, the octahedra are linked by adjacent edges along two edges, forming a chain.

Magnetite (Fe_3O_4) nanoparticles in particular are frequently employed due to their biocompatibility, high magnetic susceptibility, chemical stability, harmlessness, high saturation magnetization, and inexpensive cost.

Magnetite has a cubic inverted spinel structure packed along the [1, 1, 1] plane, with Fe^{2+} and Fe^{3+} occupying octahedral lattice cavities and Fe^{3+} occupying tetrahedral lattice cavities, as depicted in Figure 2. The formula is Fe_3+(A)[Fe_2+Fe_3+](B)O4, where A is tetrahedral and B is octahedral. Rapid electron jumps at octahedral sites between Fe^{2+} and Fe^{3+} ions can boost magnetite conductivity [64].

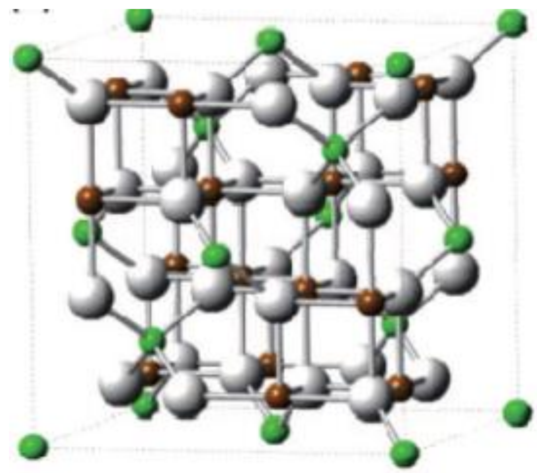

Figure 2. Fe_3O_4 crystal structure, with the green atom representing Fe^{2+}, the brown atom representing Fe^{3+}, and the white atom representing O [65].

Anbari et al. (2016) [66] carried out the photocatalyst procedure with Fe_3O_4. His research proved the monitoring of the decolorization rate of a reactive blue dye (Cibacron Blue FN-R) and variations in ORP, Ec, and solution pH by employing Fe_3O_4 as a photocatalyst under sunlight irradiation rather than a UV lamp and analyzing dye degradation. The influence of operational parameters such as pH, initial dye concentration, catalyst dose, and H_2O_2 concentration on dye decolorization efficiency was investigated.

Adsorption of dye on Fe_3O_4 was performed in a dark environment (without exposure to sunlight) by mixing the dye solution with the catalyst in a 500 mL beaker. The dye concentration is evaluated by removing samples from these beakers on a regular basis. Figure 5 shows the effects of red dye adsorption on Fe_3O_4 via the dark reaction.

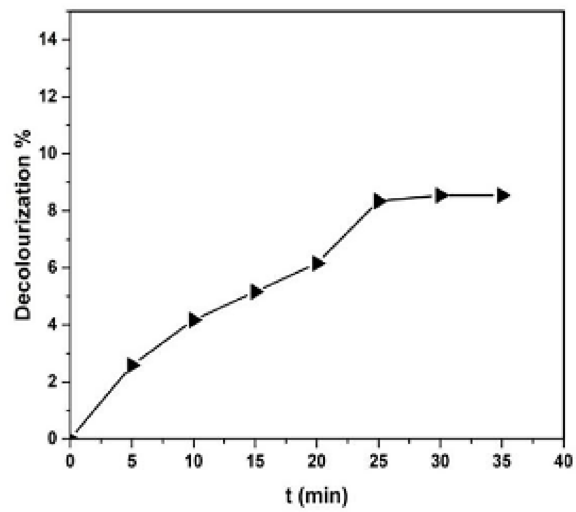

Figure 3. Adsorption of red dye on Fe_3O_4 via the dark reaction [66].

Figure 3 depicts the time-dependent fluctuation in percent decolorization owing to adsorption onto the Fe_3O_4 surface. It is obvious that the time necessary for adsorption is approximately 25 minutes. Furthermore, the experimental results revealed that the optimal pH value for solar photocatalytic Fe_3O_4 was 6.5 and the best catalysis dose was 300mg/L. Figure 4 depicts the changes in ORP, Ec (electrical conductivity), and pH of the solution during the course of the experiment with pH = 6.5. On the other hand, the ORP value increases from roughly 236 mV to 346 mV, showing that the oxidation activity increases during the reaction time; comparable results were reported by Wu and Wang, 2012 [67]. Furthermore, for Fe_3O_4, the most efficient H_2O_2 concentration is 200 mg/L. The decolorization effectiveness of reactive red dye utilizing Fe_3O_4 under sun radiation is around 85.51%.

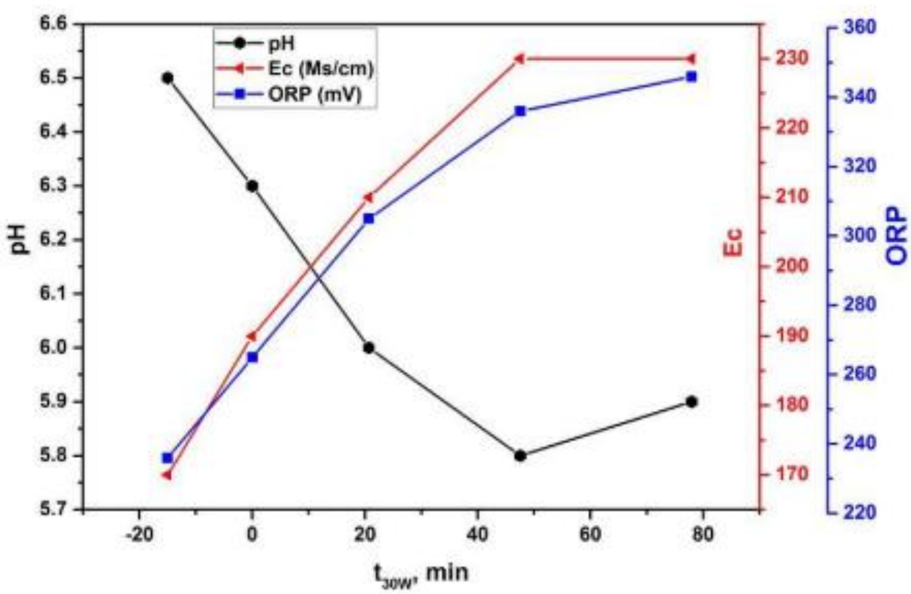

Figure 4. shows how the solution's ORP, pH, and Ec values change with exposure time

Fe_3O_4 Photocatalyst Modified With TiO_2 As A Water Controller

The development of magnetite-based nano photocatalyst materials is currently a hot research issue. The utilization of iron oxide nanocomposites as ferromagnetic materials is critical due to their novel characteristics, biocompatibility, and low cost. Magnetic semiconductor photocatalysts have strong chemical and structural stability, good magnetic characteristics, a narrow band gap, active visible light, and potential electrical performance [68].

TiO_2 nanoparticles combined with magnetics have superparamagnetic capabilities that can be easily collected, separated, or repaired by applying an external supermagnet [69]. Furthermore, charge transfer and spin can occur at the magnetic surface/catalytically active chaperone (TiO_2) interface, allowing for further tweaking of its catalytic characteristics [70], [71].

In environmental applications, TiO_2 is the most commonly used photocatalyst. However, TiO_2 has significant limitations when it comes to separation from aqueous solutions [72]. Doping magnetic materials can thus be employed to facilitate photocatalyst recovery in a magnetic field. The magnetic substance can be iron oxide or Fe_3O_4. Furthermore, the recombination of conduction electrons (e) and holes (h^+) limits the function of the photocatalysis process. To overcome this constraint, electron acceptors are typically utilized in processes involving conduction electrons. Among the electron acceptors, oxygen, hydrogen peroxide, and persulfate have been frequently employed in photocatalytic degradation [73]-[76]. Tabel 3 shows an example of employing Fe_3O_4 photocatalyst with TiO_2.

Tabel 3. Use of Fe_3O_4 photocatalyst modified by TiO_2

Material	Synthesis Method	Target Polutan	Research result	Ref
Nanocomposite TiO_2/Fe_3O_4	Coprecipitation	Methylene Orange	Fe_3O_4 nanoparticles were synthesized using the coprecipitation method and modified with TiO_2 to obtain nanocomposites. SEM analysis revealed aggregation of magnetite particles. However, the addition of TiO_2 reduces magnetite aggregation. Nevertheless, it was concluded that increasing the amount of magnetite decreased the crystal size and band gap of TiO_2 in the nanocomposite. The lower bandgap and smaller TiO_2 crystal size in the TiO_2 (0.2) Fe_3O_4(0.8) nanocomposite resulted in the best photocatalytic activity (60%) among other samples in the degradation of methylene orange.	[77]
Magneto-plasmonic Au-Ag NPs- decorated TiO_2- modified Fe_3O_4 nanocomposite	Coprecipitation, thermal and laser assisted reduction	Textile waste dyes	The results show that compared with magnetic TiO_2, the mono- and bi-plasmonic alloy photocatalysts reveal more efficient photocatalytic activity due to the presence of one/two SPR-generated hot electrons from the	[78]

Material	Synthesis Method	Target Polutan	Research result	Ref
			excited Au/Ag shell under simulated solar light irradiation. Thus Au-Ag/ TiO_2/Fe_3O_4 ternary NPs revealed 4 times more photocatalytic activity under xenon lamp irradiation. The influence of different parameters such as photocatalyst type, pH and photocatalyst dosage on the degradation efficiency of Rh_6G was investigated and reusability studies revealed only a slight decrease (below 8%) in the photocatalytic performance of the catalyst after carrying out five consecutive cycles.	
rGO-Fe_3O_4/TiO_2	Hydrothermal	methylene blue	The incorporation of rGO-Fe_3O_4 into TiO_2 shifts the light absorption of TiO_2 from the ultraviolet (UV) to the visible region. The band gap energy of the photocatalyst synthesized by rGO-Fe_3O_4/TiO_2 is reduced to 2.6 eV compared to TiO_2 (3.2 eV) which shifts the light absorption to the visible region to utilize solar energy effectively. The rGO- Fe_3O_4/TiO_2 photocatalyst showed commendable photocatalytic efficiency (99%) compared to pure TiO2 (67%) under visible light in 55 min for MG degradation	[79]
$Fe_3O_4/SiO_2/$ TiO_2/rGO magnetic nanoparticles	Hummer and coprecipitation	2,4-Dinitrophenol	On the magnetic photocatalyst $Fe_3O_4/SiO_2/TiO_2$/rGO was synthesized for the degradation of 2,4-DNP. A low-pressure UV-C lamp is used as the irradiation source. It was found that acidic conditions were more desirable for the oxidation process. TOC analysis illustrates that this process has good efficiency in 2,4-DNP mineralization, where TOC removal reached 53.04%.	[80]
$Fe_3O_4/SiO_2/TiO_2$	Coprecipitation and sol gel	Methylene blue (MB), ciprofloxacin (CIP), norfloxacin (NOR) and ibuprofen (IBP)	XRD results show that $Fe_3O_4/SiO_2/TiO_2$ calcined at 600 ^oC shows a higher anatase content. In good agreement, these particles showed the highest efficiency in the degradation of CIP, NOR, and MB, reaching complete degradation after 90 min under UV. Since IBP is considered a recalcitrant drug, only	[81]

Material	Synthesis Method	Target Polutan	Research result	Ref
			60% degradation was achieved under the same conditions. Good photocatalytic performance, efficient magnetic separation and efficient reuse of $Fe_3O_4/SiO_2/TiO_2$ have been demonstrated in multi-run experiments. Furthermore, the resulting material was proven to be an efficient catalyst against different micropollutants.	
Nanocomposite Fe_3O_4-TiO_2/graphene	Hydrothermal	Pesticide	The Fe_3O_4-TiO_2/rGO nanocomposite showed efficient peroxidase-like catalytic activity throughout the oxidation of 3,3',5,5'-tetramethylbenzidine (TMB) as a peroxidase substrate to a blue-colored oxidized product (oxTMB) in the presence of H_2O_2. Based on these observations, colorimetric detection technique was applied for sensing of atrazine as a model pesticide using TMB as the eroxidase substrate molecule and 2.98 g/L limit of detection (LOD) was obtained in the linear range of 2 to 20 g/L.	[82]
Fe_3O_4/TiO_2	Coprecipitation and sol gel	Phenol	The saturation magnetization of the magnetic is 64.68 emu g−1 and the remanence and coercivity are close to zero, indicating superparamagnetism of the prepared Fe3O4 magnetic nanoparticles. They have a spherical structure with an average particle size of 10 nm. The Fe_3O_4/TiO_2 photocatalyst was successfully prepared using the sol-gel method. The absorption threshold of the catalyst has a significant red shift, and the band gap energies of TiO_2 and Fe_3O_4/TiO_2 are 2.96 and 1.39 eV, respectively. The saturation magnetization of Fe_3O_4/TiO_2 is 1.74 emu g−1, but it can be separated quickly from solution. The as-prepared Fe_3O_4/TiO_2 photocatalyst has a clear core-shell structure with a particle size of about 20 nm. The photocatalytic degradation rate of 100 mg L−1 phenol by Fe_3O_4/TiO_2 photocatalyst was above 99% after 150 min.	[83]

Figure 5 depicts the properties of the morphological condition of the Fe_3O_4/TiO_2 photocatalyst material examined [84].

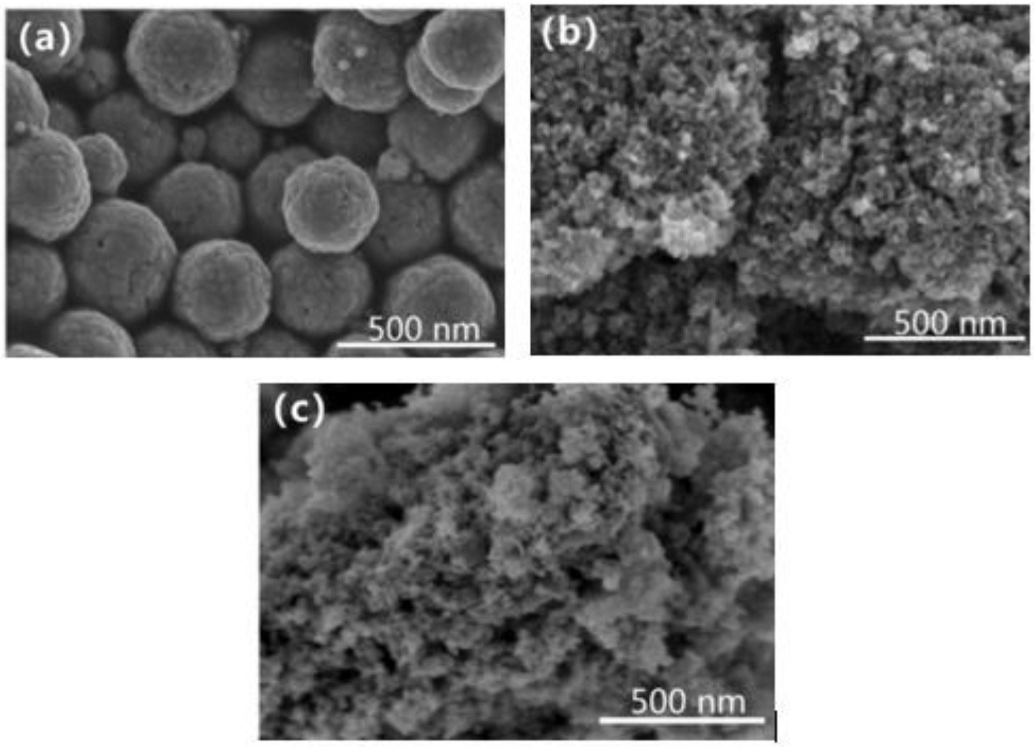

Figure 5. FESEM on a) Fe_3O_4, b) TiO_2, and c) Fe_3O_4/TiO_2

Figure 5 depicts the morphological characteristics of Fe_3O_4, TiO_2, and Fe_3O_4/TiO_2. Fe_3O_4, TiO_2, and Fe_3O_4/TiO_2 particle sizes are around 390 nm, 100 nm, and 120 nm, respectively. Although the particle size of Fe_3O_4/TiO_2 and TiO_2 is consistent, particle agglomeration occurs. This demonstrates that agglomeration can be generated by unequal joining of Fe_3O_4 and TiO_2 particles. Meanwhile, the surface area of Fe_3O_4, TiO_2, and Fe_3O_4/TiO_2 can be estimated using the BET data shown in Table 4.

Table 4. Measurement of surface area, average pore diameter and pore volume of TiO_2, Fe_3O_4/TiO_2, and Fe_3O_4 using BET [72].

Material Characteristics	Surface Area (M^2/g)	Pore Size Is Typical (Nm)	Volume Pore (Cm^3/g)
TiO_2	35.3	45.1	24.76
Fe_3O_4	34.89	28.6	35.2
Fe_3O_4/TiO_2	0.2566	0.2821	0.2151

Table 5 displays the findings of the BET analysis. TiO_2 has a surface area and pore volume of 35.3 m^2/g and 0.2566 cm^3/g, respectively, which are lowered to 24.76 m^2/g and 0.2151 cm^3/g by coating Fe_3O_4 onto TiO_2. Magnetic nanoparticles supported by TiO_2 generate this decrease in surface area and pore volume. Three nanoparticles, on the other hand, had pores smaller than 40 nm, indicating mesoporous particles. Mesoporous particles range in size from 2 to 50 nm [85, 86].

In addition, nature degrades contaminants in water; Figure 8 depicts the photodegradation mechanism process in Fe_3O_4/TiO_2.

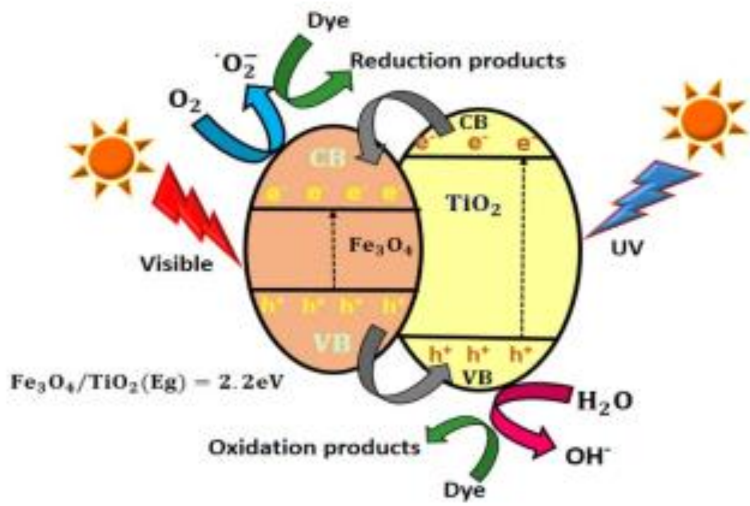

Figure 6. llustration of the photodegradation mechanism in Fe_3O_4/TiO_2 [40]

Figure 6 depicts the photodegradation process of methylene blue by Fe_3O_4/TiO_2 thin films. When exposed to direct solar radiation, electron-hole pairs are formed in Fe_3O_4. TiO_2 generates electron-hole pairs concurrently with UV absorption of sunlight. Electrons (e) from TiO_2's Conduction band (CB) migrate to Fe_3O_4's CB. Similarly, holes (h+) from the valance band (VB) of Fe_3O_4 migrate to the VB of TiO_2, resulting in effective charge separation and a drop in the recombination rate. The excited electrons react with oxygen molecules to create superoxide (O_2), which participates in the color reduction process. Similarly, holes react with water molecules to create hydroxyl ions (OH), which participate in the dye oxidation process [17], [87].

Experimental Method

Organic dyes used mostly in the textile, printing, paint, and paper sectors have been identified as a serious threat to global water systems. Silicon dioxide (SiO_2) is the ideal mesoporous support material for increasing the surface area of titania in photocatalytic applications. Silica has been widely researched for usage as a support material. Silica-supported titania composite systems have been used in applications such as green catalysis, organic synthesis, fuel desulfurization, and anti-corrosion coatings [88-91]. Because of its broad band gap, silica can also help to improve photocatalytic activity by inhibiting the development of recombination centres [92]. Aside from that, the addition of iron oxide (Fe_3O_4) to SiO_2 and TiO_2 photocatalyst materials increases their exceptional superparamagnetic and catalytic capabilities. TiO_2 composite systems with SiO_2 and Fe_3O_4 have been synthesised and exploited for photocatalytic applications in a number of recent investigations [93]. Abbas et al. (2014) used a Fe_3O_4-TiO_2 photocatalyst and UV light to degrade 5 x10-3 mol/L methylene blue (MB) dye by feeding a high catalyst concentration of 50 g/L [94], while Wu et al. (2011) obtained a Fe_3O_4-TiO_2 photocatalyst capable of removing 50%-60% of MB after 90 minutes of reaction under UV light

[95]. Xue et al. (2013) also conducted research on the $Fe_3O_4/TiO_2/SiO_2$ photocatalyst. In his study, $Fe_3O_4/TiO_2/SiO_2$ was applied to garbage in the form of methylene orange (MO).

Coprecipitation Method

Coprecipitation is a bottom-up synthesis process for producing small, nanometer-sized particles [98]. The principle of this procedure is to remove the continuous bonds of a metal complex in liquid form without taking into account the precise mechanism that occurs. The coprecipitation method is used to separate solid material from aqueous precipitate [99]. As a result, this approach is well-suited for use in the synthesis of metal materials such as zinc (Zn), titanium (Ti), and iron (Fe) [100]. In the product creation process, the coprecipitation process requires managing the pH, temperature, and stirring speed [110]. According to Ningsih [110], this method has two advantages: (1) homogenization of the reactant sediment to reduce temperature and (2) a longer process to detect metal oxide powder. The method then has three flaws: (1) it is not fast enough to create material with a high purity, (2) it does not run smoothly because the reactant used is not consistent, and (3) it lacks a universal symbiotic condition for the creation of several metal oxide.

Result and Discussion

The photocatalyst is constructed of Fe_3O_4 catalyst material with SiO_2 and a coating of TiO_2 material. The application of polluted water for photocatalytic activity employs methylene orange (MO) dye and direct UV light irradiation. In his study, $Fe_3O_4/TiO_2/SiO_2$ was applied to garbage in the form of methylene orange (MO). Figure 7 depicts the morphological condition of $Fe_3O_4/TiO_2/SiO_2$.

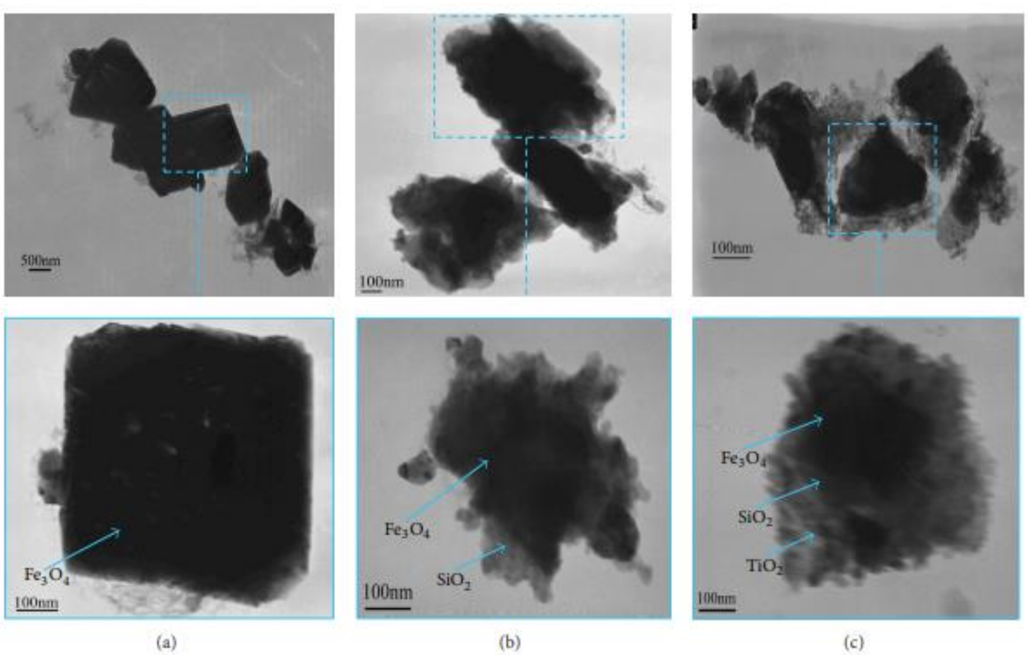

Figure 7. TEM results on (a) Fe_3O_4, (b) Fe_3O_4/SiO_2, (c) $Fe_3O_4/TiO_2/SiO_2$ [96].

Figure 7 depicts the TEM pictures of the three samples. Figure 7 (a) shows a TEM picture of Fe_3O_4 particles. The particles are clearly cubic, with diameters of roughly 700 nm. There is still some carbon around the particles. Carbon can prevent Fe_3O_4 particles from oxidising to Fe_2O_3. Figure 7(b) shows a TEM picture of Fe_3O_4/SiO_2 particles. Figure 7 clearly shows a very thin layer surrounding the black contrast Fe_3O_4 particles, which is most likely the SiO_2 layer. It can be noticed that the dispersion of Fe_3O_4/SiO_2 particles is better than that of Fe_3O_4 particles. Figure 7(c) shows a TEM picture of $Fe_3O_4/SiO_2/TiO_2$ particles. The Fe_3O_4/SiO_2 particles are clearly contained by a TiO_2 layer made up of several tiny spherical particles.

The research results demonstrate that layer by layer $Fe_3O_4/SiO_2/TiO_2$ particles were successfully generated. The photocatalysis efficiency of $Fe_3O_4/SiO_2/TiO_2$ particles is strongly connected to their specific surface area, which is 55 m^2/g. Aside from particle size and surface area, there is a band gap energy value that determines the photocatalyst's properties; the lower the band gap energy value, the more effective the photocatalyst. This is because the energy required to excite an electron from the valence band to the conduction band is lower. Even though catalyst materials have tiny band gap values, electron recombination processes are common. However, due of the existence of a SiO_2 layer between Fe_3O_4 and TiO_2, the electron recombination process can also be minimised in the $Fe_3O_4/SiO_2/TiO_2$ material. Table 6 displays the band gap values for the $Fe_3O_4/SiO_2/TiO_2$ material:

Table 6. Shows the band gap in the $Fe_3O_4/SiO_2/TiO_2$ photocatalyst [97].

Material	Band Gap (eV)
Fe_3O_4/TiO_2	2,5369
$Fe_3O_4/SiO_2/TiO_2$	1,9125

Figure 8 depicts the $Fe_3O_4/SiO_2/TiO_2$ photocatalyst process for MO degradation

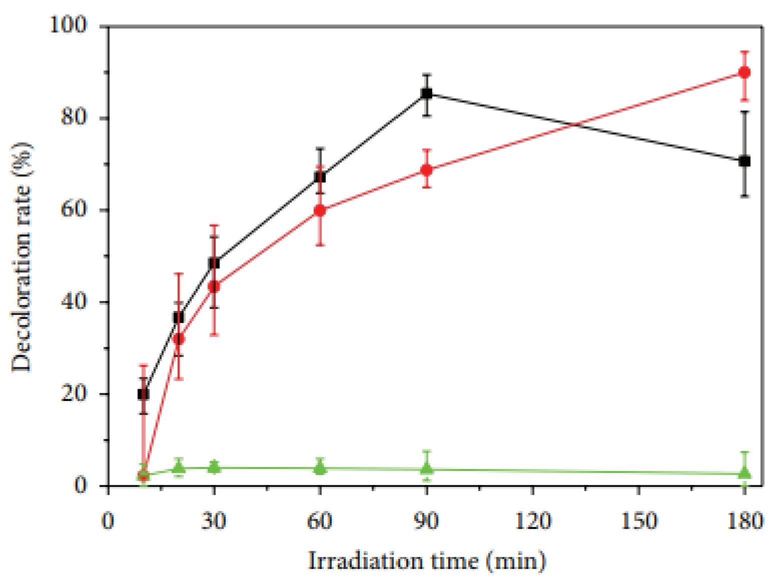

Figure 8. Relationship between irradiation time and decoloration rate of MO treated with $Fe_3O_4/SiO_2/TiO_2$ particles (red line) under UV light [96].

Figure 8 depicts the connection between irradiation time and decoloration rate of a MO solution infused with $Fe_3O_4/SiO_2/TiO_2$ particles under UV light. After 180 minutes of UV light irritation, the decoloration rate of the MO solution on $Fe_3O_4/SiO_2/TiO_2$ particles was 90%. Because the photocatalytic activity of $Fe_3O_4/SiO_2/TiO_2$ functional particles is greater when exposed to ultraviolet light, it may be assumed that $Fe_3O_4/SiO_2/TiO_2$ functional particles have a high photocatalytic activity when exposed to longer wavelength light. The photocatalytic activity of $Fe_3O_4/SiO_2/TiO_2$ functional particles under visible light irradiation is greater than under UV light irradiation, which has crucial implications for future applications.

Conclusion

Using the Coprecipitation Method, we successfully reviewed the usage of Fe3O4/SiO2/TiO2 photocatalysts as water pollution controllers. According to the TEM data, which reveal that layers of $Fe_3O_4/SiO_2/TiO_2$ particles are successfully formed because they are encased by layers of TiO_2 made up of numerous small spherical particles. Surface area in Fe_3O_4/TiO_2 and $Fe_3O_4/SiO_2/TiO_2$ is 24.76 m2/g and 55 m2/g, respectively. In the degradation process, $Fe_3O_4/SiO_2/TiO_2$ is able to degrade pollutants such as methylene orange in water through the photocatalyst process, where the results of the photocatalyst process carried out by $Fe_3O_4/SiO_2/TiO_2$ reach 90% in 180 minutes of UV light irritation. Therefore, $Fe_3O_4/SiO_2/TiO_2$ can be used as a photocatalyst for water pollution degradation.

References

[1] A. Boretti and L. Rosa, "Reassessing the projections of the World Water Development Report," *npj Clean Water*, vol. 2, no. 1, 2019, doi: 10.1038/s41545-019-0039-9.

[2] B. K. Mishra, P. Kumar, C. Saraswat, S. Chakraborty, and A. Gautam, "Water Security in a Changing Environment : Concept ," *Water*, vol. 13, no. 4, p. 490, 2021.

[3] S. Sunaryono *et al.*, "The effect of Fe3O4concentration to photocatalytic activity of Fe3O4@TiO2-PVP core-shell nanocomposite," *J. Phys. Conf. Ser.*, vol. 1595, no. 1, 2020, doi: 10.1088/1742-6596/1595/1/012003.

[4] N. Agustina, Chandra, and M. F. Aquarista, "The Quality of Water Swamp on Complaints Health Villagers," *J. Kesehat.*, vol. 12, no. 2, pp. 220–227, 2021.

[5] A. Pramono, S. Sisno, and M. Sholichin, "Study of Water Management Development in Petung Swamp Areas at the Province of East Kalimantan," *Civ. Environ. Sci.*, vol. 004, no. 02, pp. 173–182, 2021, doi: 10.21776/ub.civense.2021.00402.7.

[6] M. R. Ridho, D. Puspitasari, and I. W. A. Khrisnawan Firdaus, "the Effect of Peat Swamp Water on Tooth Demineralization of Copper and Selenium Ion," *Dentino J. Kedokt. Gigi*, vol. 5, no. 2, p. 115, 2020, doi: 10.20527/dentino.v5i2.8947.

[7] Masthura and E. Jumiati, "Peningkatan Kualitas Air Menggunakan Metode Quality Improvement of Water Using," *FISITEK J. Ilmu Fis. dan Teknol.*, vol. 1, no. 2, pp. 1–6, 2017.

[8] A. F. Anggana and P. D. Susanti, "Evaluation of water quality in the swamp river border using water quality index," *J. Degrad. Min. L. Manag.*, vol. 7, no. 4, pp. 2373–

2379, 2020, doi: 10.15243/jdmlm.

[9] S. N. Aida and A. D. Utomo, "Kajian Kualitas Perairan Untuk Perikanan Di Rawa Pening Jawa Tengah," *BAWAL Widya Ris. Perikan. Tangkap*, vol. 8, no. 3, p. 173, 2017, doi: 10.15578/bawal.8.3.2016.173-182.

[10] J. Mateo-Sagasta, S. Marjani, H. Turral, and J. Burke, *Water pollution from agriculture: a global review*. 2017. [Online]. Available: http://www.fao.org/3/a-i7754e.pdf

[11] S. Khalid *et al.*, "A review of environmental contamination and health risk assessment of wastewater use for crop irrigation with a focus on low and high-income countries," *Int. J. Environ. Res. Public Health*, vol. 15, no. 5, pp. 1–36, 2018, doi: 10.3390/ijerph15050895.

[12] G. Roviello *et al.*, "Hybrid geopolymeric foams for the removal of metallic ions from aqueous waste solutions," *Materials (Basel).*, vol. 12, no. 24, p. 4091, 2019, doi: 10.3390/ma12244091.

[13] R. Teschke, "Aluminum, Arsenic, Beryllium, Cadmium, Chromium, Cobalt, Copper, Iron, Lead, Mercury, Molybdenum, Nickel, Platinum, Thallium, Titanium, Vanadium, and Zinc: Molecular Aspects in Experimental Liver Injury," *Int. J. Mol. Sci.*, vol. 23, no. 20, 2022, doi: 10.3390/ijms232012213.

[14] S. Hayet, K. M. Sujan, A. Mustari, and M. A. Miah, "Hemato-biochemical profile of turkey birds selected from Sherpur district of Bangladesh," *Int. J. Adv. Res. Biol. Sci*, vol. 8, no. 6, pp. 1–5, 2021, doi: 10.22192/ijarbs.

[15] M. Frankowski, "Simultaneous determination of inorganic and organic ions in plant parts of Betula pendula from two different types of ecosystems (Wielkopolski National Park and Chemical Plant in Luboń, Poland)," *Environ. Sci. Pollut. Res.*, vol. 23, no. 11, pp. 11046–11057, 2016, doi: 10.1007/s11356-016-6274-4.

[16] Y. B. Yuliyati, S. Listiani, S. Solihudin, and A. R. Noviyanti, "Isolation of Silica-Lignin Composites from Rice Husk and Their Adsorption to Cr(VI)," *ALCHEMY J. Penelit. Kim.*, vol. 14, no. 2, p. 267, 2018, doi: 10.20961/alchemy.14.2.19818.267-276.

[17] P. B. Tchounwou, C. G. Yedjou, A. K. Patlolla, and D. J. Sutton, "Molecular, clinical and environmental toxicicology Volume 3: Environmental Toxicology," *Mol. Clin. Environ. Toxicol.*, vol. 101, pp. 133–164, 2012, doi: 10.1007/978-3-7643-8340-4.

[18] K. S. Shafaqat *et al.*, "Heavy Metals Contamination and what are the Impacts on Living Organisms," *Greener J. Environ. Manag. Public Saf.*, vol. 2, no. 4, pp. 2354–2276, 2013, [Online]. Available: www.gjournals.org

[19] S. Mitra *et al.*, "Impact of heavy metals on the environment and human health: Novel therapeutic insights to counter the toxicity," *J. King Saud Univ. - Sci.*, vol. 34, no. 3, p. 101865, 2022, doi: 10.1016/j.jksus.2022.101865.

[20] M. Jaishankar, T. Tseten, N. Anbalagan, B. B. Mathew, and K. N. Beeregowda, "Toxicity, mechanism and health effects of some heavy metals," *Interdiscip. Toxicol.*, vol. 7, no. 2, pp. 60–72, 2014, doi: 10.2478/intox-2014-0009.

[21] R. Erdoo Kukwa, D. Tyoker Kukwa, A. David Oklo, T. Thaddeus Ligom, B. Ishwah, and J. Ajegi Omenka, "Adsorption Studies of Silica Adsorbent Using Rice Husk as a Base Material for Metal Ions Removal from Aqueous Solution," *Am. J. Chem. Eng.*, vol. 8, no. 2, p. 48, 2020, doi: 10.11648/j.ajche.20200802.12.

[22] P. Wang *et al.*, "Silica coated Fe3O4 magnetic nanospheres for high removal of organic pollutants from wastewater," *Chem. Eng. J.*, vol. 306, pp. 280–288, 2016, doi: 10.1016/j.cej.2016.07.068.

[23] V. K. Gupta, I. Ali, T. A. Saleh, A. Nayak, and S. Agarwal, "Chemical treatment technologies for waste-water recycling - An overview," *RSC Adv.*, vol. 2, no. 16, pp. 6380–6388, 2012, doi: 10.1039/c2ra20340e.

[24] W. J. Cosgrove and D. P. Loucks, "Water management: Current and future challenges and research directions," *Water Resour. Res.*, vol. 51, no. 6, pp. 4823–4839, 2015, doi: 10.1002/2014WR016869.Received.

[25] A. K. Mishra, *Smart Materials For Waste Water Applications*, vol. 4. 2016.

[26] G. Ren *et al.*, "Recent advances of photocatalytic application in water treatment: A review," *Nanomaterials*, vol. 11, no. 7, 2021, doi: 10.3390/nano11071804.

[27] S. S. Mohtar *et al.*, "Impact of doping and additive applications on photocatalyst textural properties in removing organic pollutants: A review," *Catalysts*, vol. 11, no. 10, pp. 1–30, 2021, doi: 10.3390/catal11101160.

[28] M. Sakar, R. Mithun Prakash, and D. Trong-On, "Insights into the tio2-based photocatalytic systems and their mechanisms," *Catalysts*, vol. 9, no. 8, 2019, doi: 10.3390/catal9080680.

[29] M. Ge *et al.*, "A review of one-dimensional TiO2 nanostructured materials for environmental and energy applications," *J. Mater. Chem. A*, vol. 4, no. 18, pp. 6772–6801, 2016, doi: 10.1039/c5ta09323f.

[30] B. Liu, B. Chen, and B. Zhang, "Oily wastewater treatment by nano-TiO_2-induced photocatalysis," *IEEE Nanotechnol. Mag.*, no. July, pp. 2–13, 2017.

[31] Z. Li, X. Meng, and Z. Zhang, "Fewer-layer BN nanosheets-deposited on Bi 2 MoO 6 microspheres with enhanced visible light-driven photocatalytic activity," *Appl. Surf. Sci.*, vol. 483, no. March, pp. 572–580, 2019, doi: 10.1016/j.apsusc.2019.03.245.

[32] Q. Lin *et al.*, "Self-cleaning photocatalytic MXene composite membrane for synergistically enhanced water treatment: Oil/water separation and dyes removal," *Chem. Eng. J.*, vol. 427, no. July 2021, p. 131668, 2022, doi: 10.1016/j.cej.2021.131668.

[33] R. Yang *et al.*, "One-step preparation (3D/2D/2D) BiVO4/FeVO4@rGO heterojunction composite photocatalyst for the removal of tetracycline and hexavalent chromium ions in water," *Chem. Eng. J.*, vol. 390, no. February, p. 124522, 2020, doi: 10.1016/j.cej.2020.124522.

[34] Y. Tang, G. Zhang, C. Liu, S. Luo, and X. Xu, "Magnetic TiO2-graphene composite as a high-performance and recyclable platform for efficient photocatalytic removal of

herbicides from water," *J. Hazard. Mater.*, vol. 252–253, pp. 115–122, 2013, doi: 10.1016/j.jhazmat.2013.02.053.

[35] Z. Zhang *et al.*, "Synthesis of ag loaded ZnO/BiOCl with high photocatalytic performance for the removal of antibiotic pollutants," *Crystals*, vol. 11, no. 8, pp. 1–12, 2021, doi: 10.3390/cryst11080981.

[36] J. Liu *et al.*, "Highly efficient photocatalytic degradation of oil pollutants by oxygen deficient SnO2 quantum dots for water remediation," *Chem. Eng. J.*, vol. 404, 2021, doi: 10.1016/j.cej.2020.127146.

[37] Q. Zhou *et al.*, "Novel hierarchical carbon quantum dots-decorated BiOCl nanosheet/carbonized eggshell membrane composites for improved removal of organic contaminants from water via synergistic adsorption and photocatalysis," *Chem. Eng. J.*, vol. 420, no. P1, p. 129582, 2021, doi: 10.1016/j.cej.2021.129582.

[38] S. Wu, X. Yu, J. Zhang, Y. Zhang, Y. Zhu, and M. Zhu, "Construction of BiOCl/CuBi2O4 S-scheme heterojunction with oxygen vacancy for enhanced photocatalytic diclofenac degradation and nitric oxide removal," *Chem. Eng. J.*, vol. 411, no. November 2020, p. 128555, 2021, doi: 10.1016/j.cej.2021.128555.

[39] M. P. Ravikumar, S. Bharathkumar, B. Urupalli, M. K. Murikinati, S. M. Venkatakrishnan, and S. Mohan, "Insights into the Photocatalytic Memory Effect of Magneto- Plasmonic Ag−Fe3O4@TiO2 Ternary Nanocomposites for Dye degradation and H2 Production under light and dark Conditions," *Energy and Fuels*, vol. 36, no. 19, pp. 11503–11514, 2022, doi: 10.1021/acs.energyfuels.2c01563.

[40] G. Shilpa, P. M. Kumar, P. R. Deepthi, A. Sukhdev, P. Bhaskar, and D. K. Kumar, "Improved Photocatalytic Performance of Fe3O4/TiO2 Thin Film in the Degradation of MB Dye Under Sunlight Radiation," *Brazilian J. Phys.*, vol. 53, no. 2, pp. 1–8, 2023, doi: 10.1007/s13538-022-01243-z.

[41] A. Babyszko, A. Wanag, M. Sadłowski, E. Kusiak-Nejman, and A. W. Morawski, "Synthesis and Characterization of SiO2/TiO2 as Photocatalyst on Methylene Blue Degradation," *Catalysts*, vol. 12, no. 11, 2022, doi: 10.3390/catal12111372.

[42] S. M. Gupta and M. Tripathi, "A review of TiO2 nanoparticles," *Chinese Sci. Bull.*, vol. 56, no. 16, pp. 1639–1657, 2011, doi: 10.1007/s11434-011-4476-1.

[43] B. Minhas, S. Dino, Y. Zuo, H. Qian, and X. Zhao, "Improvement of corrosion resistance of tio2 layers in strong acidic solutions by anodizing and thermal oxidation treatment," *Materials (Basel).*, vol. 14, no. 5, pp. 1–13, 2021, doi: 10.3390/ma14051188.

[44] R. Das, V. Ambardekar, and P. P. Bandyopadhyay, "Titanium Dioxide and Its Applications in Mechanical, Electrical, Optical, and Biomedical Fields," *Intech*, vol. 11, no. tourism, p. 13, 2016, [Online]. Available: https://www.intechopen.com/books/advanced-biometric-technologies/liveness-detection-in-biometrics

[45] M. Ibrahim, J. B. Agboola, S. A. Abdulkareem, O. Adedipe, and J. O. Tijani, "Effects of elevated temperature on the corrosion resistance of silver–cobalt oxide–titanium

dioxide (Ag/Co3O4/TiO2) nanocomposites coating on AISI 1020," *Sci. Rep.*, vol. 11, no. 1, pp. 1–14, 2021, doi: 10.1038/s41598-021-90272-w.

[46] M. Ge, Z. Hu, J. Wei, Q. He, and Z. He, "Recent advances in persulfate-assisted TiO2-based photocatalysis for wastewater treatment: Performances, mechanism and perspectives," *J. Alloys Compd.*, vol. 888, p. 161625, 2021, doi: 10.1016/j.jallcom.2021.161625.

[47] C. B. Anucha, I. Altin, E. Bacaksiz, and V. N. Stathopoulos, "Titanium dioxide (TiO_2)-based photocatalyst materials activity enhancement for contaminants of emerging concern (CECs) degradation: In the light of modification strategies," *Chem. Eng. J. Adv.*, vol. 10, no. September 2021, p. 100262, 2022, doi: 10.1016/j.ceja.2022.100262.

[48] S. Sagadevan *et al.*, "Photocatalytic Efficiency of Titanium Dioxide for Dyes and Heavy Metals Removal from Wastewater," *Bull. Chem. React. Eng. Catal.*, vol. 17, no. 2, pp. 430–450, 2022, doi: 10.9767/BCREC.17.2.13948.430-450.

[49] Y. Zhang *et al.*, "Titanate and titania nanostructured materials for environmental and energy applications: A review," *RSC Adv.*, vol. 5, no. 97, pp. 79479–79510, 2015, doi: 10.1039/c5ra11298b.

[50] M. Pelaez *et al.*, "A review on the visible light active titanium dioxide photocatalysts for environmental applications," *Appl. Catal. B Environ.*, vol. 125, pp. 331–349, 2012, doi: 10.1016/j.apcatb.2012.05.036.

[51] C. H. Lin and W. H. Chen, "Graphene family nanomaterials (Gfn)-tio2 for the photocatalytic removal of water and air pollutants: Synthesis, characterization, and applications," *Nanomaterials*, vol. 11, no. 12, 2021, doi: 10.3390/nano11123195.

[52] N. Rahimi, R. A. Pax, and E. M. A. Gray, "Review of functional titanium oxides. I: TiO2 and its modifications," *Prog. Solid State Chem.*, vol. 44, no. 3, pp. 86–105, 2016, doi: 10.1016/j.progsolidstchem.2016.07.002.

[53] A. J. Haider, Z. N. Jameel, and I. H. M. Al-Hussaini, "Review on: Titanium dioxide applications," *Energy Procedia*, vol. 157, pp. 17–29, 2019, doi: 10.1016/j.egypro.2018.11.159.

[54] H. N. C. Dharma *et al.*, "A Review of Titanium Dioxide (TiO2)-Based Photocatalyst for Oilfield-Produced Water Treatment," *Membranes (Basel).*, vol. 12, no. 3, 2022, doi: 10.3390/membranes12030345.

[55] R. Ceccato, "Sol-Gel Synthesis of TiO 2 Nanocrystalline Particles with Enhanced Surface Area through the Reverse Micelle Approach," vol. 2019, 2019.

[56] G. S. Falk and M. Borlaf, "Microwave-assisted synthesis of TiO 2 nanoparticles : photocatalytic activity of powders and thin films," 2018.

[57] T. Aguilar, I. Carrillo-berdugo, G. Roberto, J. Jes, C. Fern, and J. Navas, "A Solvothermal Synthesis of TiO 2 Nanoparticles in a Non-Polar Medium to Prepare Highly Stable Nanofluids with Improved Thermal Properties," 2018, doi: 10.3390/nano8100816.

[58] T. Tatarchuk, N. Danyliuk, A. Shyichuk, W. Macyk, and M. Naushad, "Photocatalytic degradation of dyes using rutile TiO 2 synthesized by reverse micelle and low temperature methods : real-time monitoring of the degradation kinetics," *J. Mol. Liq.*, vol. 342, p. 117407, 2021, doi: 10.1016/j.molliq.2021.117407.

[59] E. Ambrosio *et al.*, "Optimization of photocatalytic degradation of biodiesel using TiO2/H2O2 by experimental design," *Sci. Total Environ.*, vol. 581–582, pp. 1–9, 2017, doi: 10.1016/j.scitotenv.2016.11.177.

[60] H. Gobara, R. El-Salamony, D. Mohamed, M. Mishrif, Y. Moustafa, and T. Gendy, "Use of SiO 2 - TiO 2 Nanocomposite as Photocatalyst for the Removal of Trichlorophenol : A Kinetic Study and Numerical Evaluation," *Chem. Mater. Res.*, vol. 6, no. 6, pp. 63–82, 2014.

[61] W. Udaibah and A. Priyanto, "Synthesis and Structure Characterization of SiO2 from Petung Bamboo Leaf Ash (Dendrocalamus asper (Schult.f.) Backer ex Heyne)," *J. Nat. Sci. Math. Res.*, vol. 3, no. 1, pp. 215–220, 2017, doi: 10.21580/jnsmr.2017.3.1.1697.

[62] F. A. Chaves and D. Jiménez, "Effects and mechanism of SiO2 on photocatalysis and super hydrophilicity of TiO2 films prepared by sol-gel method," *Nanotechnology*, vol. 29, no. 27, 2018.

[63] I. M. Joni, L. Nulhakim, M. Vanitha, and C. Panatarani, "Characteristics of crystalline silica (SiO2) particles prepared by simple solution method using sodium silicate (Na2SiO3) precursor," *J. Phys. Conf. Ser.*, vol. 1080, no. 1, 2018, doi: 10.1088/1742-6596/1080/1/012006.

[64] L. S. Ganapathe, M. A. Mohamed, R. M. Yunus, and D. D. Berhanuddin, "Magnetite (Fe3O4) nanoparticles in biomedical application: From synthesis to surface functionalisation," *Magnetochemistry*, vol. 6, no. 4, pp. 1–35, 2020, doi: 10.3390/magnetochemistry6040068.

[65] S. N. Sun, C. Wei, Z. Z. Zhu, Y. L. Hou, S. S. Venkatraman, and Z. C. Xu, "Magnetic iron oxide nanoparticles: Synthesis and surface coating techniques for biomedical applications," *Chinese Phys. B*, vol. 23, no. 3, pp. 1–19, 2014, doi: 10.1088/1674-1056/23/3/037503.

[66] R. Al-anbari, A. H. Al-Obaidy, and E. Abd, "Photocatalytic activity of Fe3O4 under solar radiation," *Mesopotamia Environ. J.*, vol. 2, no. 14, pp. 41–53, 2016, doi: 10.1063/1.4914057.

[67] H. Wu and S. Wang, "Impacts of operating parameters on oxidation-reduction potential and pretreatment efficacy in the pretreatment of printing and dyeing wastewater by Fenton process," *J. Hazard. Mater.*, vol. 243, pp. 86–94, 2012, doi: 10.1016/j.jhazmat.2012.10.030.

[68] P. Mishra, S. Patnaik, and K. Parida, "An overview of recent progress on noble metal modified magnetic Fe 3 O 4 for photocatalytic pollutant degradation and H 2 evolution," *Catal. Sci. Technol.*, vol. 9, no. 4, pp. 916–941, 2019, doi: 10.1039/c8cy02462f.

[69] P. Ma *et al.*, "Synthesis and photocatalytic property of Fe3O4@TiO2 core/shell nanoparticles supported by reduced graphene oxide sheets," *J. Alloys Compd.*, vol. 578, pp. 501–506, 2013, doi: 10.1016/j.jallcom.2013.07.026.

[70] A. Nezhadali, M. R. Shapouri, and M. Amoli-Diva, "Laser and Solar Light-Induced Degradation of Pollutant Dyes Using Bi-Plasmonic Ag-Au Nanoparticles-Decorated Magnetic TiO2 for Textile Wastewater Treatment," *J. Nanostructures*, vol. 12, no. 1, pp. 45–61, 2022, doi: 10.22052/JNS.2022.01.006.

[71] L. Gnanasekaran *et al.*, "Nanosized Fe3O4 incorporated on a TiO2 surface for the enhanced photocatalytic degradation of organic pollutants," *J. Mol. Liq.*, vol. 287, 2019, doi: 10.1016/j.molliq.2019.110967.

[72] M. A. Zazouli, F. Ghanbari, M. Yousefi, and S. Madihi-Bidgoli, "Photocatalytic degradation of food dye by Fe3O4-TiO2 nanoparticles in presence of peroxymonosulfate: The effect of UV sources," *J. Environ. Chem. Eng.*, vol. 5, no. 3, pp. 2459–2468, 2017, doi: 10.1016/j.jece.2017.04.037.

[73] M. Ahmadi, F. Ghanbari, and M. Moradi, "Photocatalysis assisted by peroxymonosulfate and persulfate for benzotriazole degradation: Effect of ph on sulfate and hydroxyl radicals," *Water Sci. Technol.*, vol. 72, no. 11, pp. 2095–2102, 2015, doi: 10.2166/wst.2015.437.

[74] Y. Li, M. Zhang, M. Guo, and X. Wang, "Preparation and properties of a nano TiO2/Fe3O 4 composite superparamagnetic photocatalyst," *Rare Met.*, vol. 28, no. 5, pp. 423–427, 2009, doi: 10.1007/s12598-009-0082-7.

[75] D. Beydoun, R. Amal, G. K.-C. Low, and S. McEvoy, "Novel Photocatalyst: Titania-Coated Magnetite. Activity and Photodissolution Donia," *Phys. Chem.*, vol. 104, pp. 4387–4396, 2000.

[76] M. Ahmadi *et al.*, "Enhanced photocatalytic degradation of tetracycline and real pharmaceutical wastewater using MWCNT/TiO2 nano-composite," *J. Environ. Manage.*, vol. 186, no. 2016, pp. 55–63, 2017, doi: 10.1016/j.jenvman.2016.09.088.

[77] B. Mercyrani, R. Hernandez-Maya, M. Solís-López, C. Th-Th, and S. Velumani, "Photocatalytic degradation of Orange G using TiO2/Fe3O4 nanocomposites," *J. Mater. Sci. Mater. Electron.*, vol. 29, no. 18, pp. 15436–15444, 2018, doi: 10.1007/s10854-018-9069-1.

[78] M. Amoli-Diva, A. Anvari, and R. Sadighi-Bonabi, "Synthesis of magneto-plasmonic Au-Ag NPs-decorated TiO2-modified Fe3O4 nanocomposite with enhanced laser/solar-driven photocatalytic activity for degradation of dye pollutant in textile wastewater," *Ceram. Int.*, vol. 45, no. 14, pp. 17837–17846, 2019, doi: 10.1016/j.ceramint.2019.05.355.

[79] S. Bibi *et al.*, "Photocatalytic degradation of malachite green and methylene blue over reduced graphene oxide (rGO) based metal oxides (rGO-Fe3O4/TiO2) nanocomposite under UV-visible light irradiation," *J. Environ. Chem. Eng.*, vol. 9, no. 4, 2021, doi: 10.1016/j.jece.2021.105580.

[80] B. MirzaHedayat, M. Noorisepehr, E. Dehghanifard, A. Esrafili, and R. Norozi, "Evaluation of photocatalytic degradation of 2,4-Dinitrophenol from synthetic wastewater using Fe3O4@SiO2@TiO2/rGO magnetic nanoparticles," *J. Mol. Liq.*, vol. 264, no. 2017, pp. 571–578, 2018, doi: 10.1016/j.molliq.2018.05.102.

[81] S. Teixeira *et al.*, "Photocatalytic degradation of recalcitrant micropollutants by reusable Fe3O4/SiO2/TiO2 particles," *J. Photochem. Photobiol. A Chem.*, vol. 345, pp. 27–35, 2017, doi: 10.1016/j.jphotochem.2017.05.024.

[82] P. K. Boruah and M. R. Das, "Dual responsive magnetic Fe3O4-TiO2/graphene nanocomposite as an artificial nanozyme for the colorimetric detection and photodegradation of pesticide in an aqueous medium," *J. Hazard. Mater.*, vol. 385, p. 121516, 2020, doi: 10.1016/j.jhazmat.2019.121516.

[83] J. Chang, Q. Zhang, Y. Liu, Y. Shi, and Z. Qin, "Preparation of Fe3O4/TiO2 magnetic photocatalyst for photocatalytic degradation of phenol," *J. Mater. Sci. Mater. Electron.*, vol. 29, no. 10, pp. 8258–8266, 2018, doi: 10.1007/s10854-018-8832-7.

[84] L. Sun *et al.*, "Study on Photocatalytic Degradation of Acid Red 73 by Fe3O4@TiO2 Exposed (001) Facets," *Appl. Sci.*, vol. 12, no. 3574, pp. 1–11, 2022, [Online]. Available: https://www.mdpi.com/2076-3417/12/7/3574

[85] O. Pagar, H. Nagare, Y. Chine, R. Autade, P. Narode, and V. Sanklecha, "Mesoporous Silica: A Review," *Int. J. Pharm. Drug Anal.*, vol. 6, no. 1, pp. 1–12, 2018.

[86] A. Hutem and C. Yuenyao, "Characteristics of MSNs synthesized by structure directing method," *J. Phys. Conf. Ser.*, vol. 2431, no. 1, 2023, doi: 10.1088/1742-6596/2431/1/012046.

[87] N. I. M. Razip, K. M. Lee, C. W. Lai, and B. H. Ong, "Recoverability of Fe3O4/TiO2 nanocatalyst in methyl orange degradation," *Mater. Today Proc.*, vol. 27, no. xxxx, pp. 0–31, 2019, [Online]. Available: https://doi.org/10.1016/j.jare.2020.01.010%0Ahttps://doi.org/10.1016/j.nano.2021.102426%0Ahttps://doi.org/10.1080/03008207.2019.1617280%0Ahttp://dx.doi.org/10.1038/s41598-019-38972-2%0Ahttps://doi.org/10.1016/j.matpr.2019.12.188%0Ahttps://doi.org/10.1016/

[88] A. K. Guin, S. K. Nayak, T. K. Rout, N. Bandyopadhyay, and D. K. Sengupta, "Corrosion behavior of nanohybrid titania-silica composite coating on phosphated steel sheet," *J. Coatings Technol. Res.*, vol. 9, no. 1, pp. 97–106, 2012, doi: 10.1007/s11998-011-9321-6.

[89] B. Llano, M. C. Hidalgo, L. A. Rios, and J. A. Navío, "Effect of the type of acid used in the synthesis of titania-silica mixed oxides on their photocatalytic properties," *Appl. Catal. B Environ.*, vol. 150–151, pp. 389–395, 2014, doi: 10.1016/j.apcatb.2013.12.039.

[90] X. M. Yan, P. Mei, L. Xiong, L. Gao, Q. Yang, and L. Gong, "Mesoporous titania-silica-polyoxometalate nanocomposite materials for catalytic oxidation desulfurization of fuel oil," *Catal. Sci. Technol.*, vol. 3, no. 8, pp. 1985–1992, 2013, doi: 10.1039/c3cy20732c.

[91] M. B. Gawande, R. K. Pandey, and R. V. Jayaram, "Role of mixed metal oxides in catalysis science - Versatile applications in organic synthesis," *Catal. Sci. Technol.*, vol. 2, no. 6, pp. 1113–1125, 2012, doi: 10.1039/c2cy00490a.

[92] X. Yu, S. Liu, and J. Yu, "Superparamagnetic γ-Fe2O3@SiO2@TiO2 composite microspheres with superior photocatalytic properties," *Appl. Catal. B Environ.*, vol. 104, no. 1–2, pp. 12–20, 2011, doi: 10.1016/j.apcatb.2011.03.008.

[93] N. Abbas, G. N. Shao, S. M. Imran, M. S. Haider, and H. T. Kim, "Inexpensive synthesis of a high-performance Fe3O4-SiO2-TiO2 photocatalyst: Magnetic recovery and reuse," *Front. Chem. Sci. Eng.*, vol. 10, no. 3, pp. 405–416, 2016, doi: 10.1007/s11705-016-1579-x.

[94] M. Abbas, B. Parvatheeswara Rao, V. Reddy, and C. Kim, "Fe3O4/TiO2 core/shell nanocubes: Single-batch surfactantless synthesis, characterization and efficient catalysts for methylene blue degradation," *Ceram. Int.*, vol. 40, no. 7, pp. 11177–11186, 2014, doi: 10.1016/j.ceramint.2014.03.148.

[95] W. Wu, X. Xiao, S. Zhang, F. Ren, and C. Jiang, "Facile method to synthesize magnetic iron oxides/TiO 2 hybrid nanoparticles and their photodegradation application of methylene blue," *Nanoscale Res. Lett.*, vol. 6, pp. 1–15, 2011, doi: 10.1186/1556-276X-6-533.

[96] C. Xue *et al.*, "High photocatalytic activity of Fe3O4-SiO 2-TiO2 functional particles with core-shell structure," *J. Nanomater.*, vol. 2013, 2013, doi: 10.1155/2013/762423.

[97] S. Wardiyati, W. A. Adi, and D. S. Winatapura, "Pengaruh Penambahan SiO2 Terhadap Karakteristik dan Kinerja Fotokatalitik Fe3o4/Tio2 pada Degradasi Methylene Blue," *J. Kim. dan Kemasan*, vol. 38, no. 1, p. 31, 2016, doi: 10.24817/jkk.v38i1.1976.

[98] Sau, T K. Rogach, A L. (Eds.). 2012. Complex-shaped Metal Nanoparticles: Bottom-Up Syntheses and Application, Wiley-VCH Verlag & Co KgaA. Weinheim: Germany.

[99] Zhu, Ke-Rong. Zhang, Ming-Sheng. Hong, Jian-Ming. Yin, Zhen. 2005. "Size Effect on Phase Transition Sequence of TiO2 Nanocrystal". Materials Science and Engineering A 403 (2005) pp. 87–93.

[100] Ningtyas, Sri Astutik. 2010. "Sintesis Partikel Nano $ZnCo_2O_2$ denganMetode Kopresipitasi dan Karakterisasi Struktur magneto Dielektrisitasnya". Perpustakaan Digital, Universitas Negeri Malang (http://library.um.ac.id).

[110] S. K. W. Ningsih, 2016, Sintesis Anorganik, Universitas Negeri Padang.